



Towards improved integration of hydrological uncertainty and hydraulic model sensitivity in flood hazard mapping

Simon Rusjan^{1,2}, Jasna Donevska^{1,2}, Matjaž Mikoš¹

Chair of Hydrology and Hydraulic Engineering, Faculty of Civil and Geodetic Engineering, University of Ljubljana, Jamova
2, SI-1000 Ljubljana, Slovenia

² Protim Ržišnik Perc Ltd., Ljubljana, Slovenia

Correspondence to: Simon Rusjan (simon.rusjan@fgg.uni-lj.si)

Abstract

The study investigates the impact of hydrological uncertainties and the related sensitivity of the hydrodynamic modelling results on flood hazard mapping. Uncertainties in flood frequency analysis (FFA), including anticipated impact of climate change and sensitivity to channel and floodplain roughness, were examined. The study area is the lower Vipava river, a transboundary catchment shared between Slovenia and Italy with variable floodplain topography. Sensitivity analysis revealed that uncertainty in FFA and river channel roughness significantly influenced the inundation spatial extent and inundation depth, the impact of floodplain roughness appears to be limited. The analysis shows that natural successional changes in river channel roughness substantially impact the results of a 10-year return period (RP) event, increasing flood extent by 45%. The increase in inundated areas is less pronounced for 100- and 500-year RP floods, with increases of 15% and 11%, respectively. The assessed probability of inundation based on scenario ensembles provided an informative identification of areas most susceptible to potential changes in flood hazard. Our findings highlight the need to address critical scenario ensembles that incorporate FFA uncertainty and hydraulic roughness sensitivity, leading to more informative flood hazard mapping for steering future land use planning.

Keywords: design hydrograph peaks, hydrodynamic modelling, roughness conditions, scenario ensembles, inundation probability

1 Introduction

Floods are among the most common and destructive natural disasters that affect humans and society, causing significant losses and damage annually (Zahmatkesh et al., 2021). Currently, flood mapping is commonly employed method for reducing pre-impact flood hazards. Different tools and modelling approaches are used to elaborate flood hazard maps which are then integrated into spatial planning through various administrative measures. However, flood hazard mapping is subjected to significant uncertainties and is sensitive to spatial and temporal variation in hydrological and hydraulic processes, changes in land use, alterations in river channels characteristics, limited knowledge about the physical properties of the system, as well as the inevitable problem of data availability. These factors pose challenges for flood risk management (Alfonso et al., 2016;



Winter et al. 2018; Stephens & Bledsoe, 2020; Nogherotto et al., 2022, Herrera et al., 2022; Mishra et al., 2022; Paulik et al., 2024; Yu et al., 2025).

Flood hazard maps that are derived deterministically, without considering potential uncertainties, have often been shown to provide inaccurate estimates of the inundation extension. Due to the limitations of the deterministic approach to flood hazard assessment, it is crucial to quantify related uncertainties and analyze the sensitivity of resulting flood hazard mapping to hydraulic model input data (Glas et al., 2016; Smart, 2018; Stephens & Bledsoe, 2020; Bates, 2022; Hashimoto, 2023). Flood inundation and flood hazard maps, which incorporate various associated uncertainties, offer a more comprehensive evaluation of flood hazards. This enables better informed decision making and improved flood risk management (Simões et al., 2015; Zahmatkesh et al., 2021; Maranzoni et al., 2023). However, a significant knowledge gap persists in the practical consideration of uncertainty and sensitivity aspects. This is mainly because systematic methods to quantify uncertainty and sensitivity are still lacking.

Given the possibility to perform multiple simulation runs with varying input data and parameter settings, hydrodynamic models can be applied to assess various sources of uncertainties affecting flood hazard and flood risk assessments (Bates, 2022). However, the long computing times of more complex hydrodynamic models, such as those used in areas with complex terrain topography, longer river sections or various hydraulic structures limit the possibility to perform numerous simulation runs and conduct statistical analysis of the simulation results in everyday analysis of flood hazard. Furthermore, understanding hazard maps that include uncertainty in flood hazard extent can be challenging, as the way uncertainty is depicted in these maps has a significant impact on users' decision-making abilities (Lim et al. 2024; Pavesi et al., 2024). The incorporation of uncertainty and sensitivity aspects within the framework of flood hazard mapping could be improved through the utilization of a predefined scenario ensembles, which are informed by the domain knowledge pertaining to flood processes.

In this study we present a systematic approach to integrate the impact of uncertainty in input hydrological data and perform sensitivity analysis of the hydrodynamic modelling results on the extension of the inundated areas and elaboration of flood hazard mapping. The approach centres on selection of target (critical) scenario ensembles that provides improved insight into flood hazard mapping under hydrological uncertainty and hydraulic sensitivity. The research objectives of the study were the following:

- 1) Evaluate the impact of uncertainty in the FFA on hydrodynamic simulation results and the spatial extent of the inundated areas.
- 2) Analyze the sensitivity of the hydrodynamic modelling results to river channel roughness conditions and the roughness conditions on the floodplains.
- 3) Use global sensitivity analysis to identify the key drivers of inundation extent, and estimate inundation probability using scenario ensembles to support more informative flood hazard maps.



2 Methods

2.1 Study area description

65 The Vipava river is a transboundary river that flows through western Slovenia and northeast Italy. This study focuses on the lower Vipava river valley (Figure 1), which comprises the last 21 km of the river in Slovenia before it enters Italy. The total length of the Vipava river is 49 km, with 45 km of it located in Slovenia. It flows into the Soča river near the Municipality of Savogna d'Isonzo after entering Italy. The region has prevailing sub-Mediterranean climate characteristics with hot summers and mild winters (Magjar et al., 2016). The average annual precipitation in the headwater parts of the catchment surpasses 70 2,000 mm, whereas the lower region receives approximately 1,500 mm annually. The Vipava river catchment area is characterized by karst hydrology in most of its eastern and northeastern highland parts, while the central, southern, and southeastern parts are dominated by the torrential characteristics of the Vipava river tributaries (Rusjan et al., 2012).

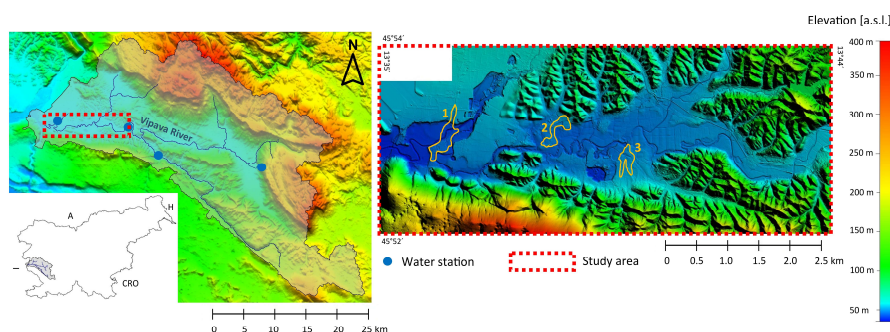


Figure 1: Location of the Vipava river catchment and the study reach. Polygons 1-3 indicate locations of larger built-up areas.

75 The area is particularly interesting for studying the uncertainty and sensitivity aspects of flood hazard assessment due to heterogeneous hydrological response of the catchment (Jelovčan and Šraj, 2022) and highly variable floodplain areas extension. In some sections of the Vipava river, the width of the inundated areas can exceed 1 km, whereas in other sub-sections, the inundated areas are constrained to the width of the main river channel due to the narrow river valley. The floodplain areas extending along the studied Vipava river section have been significantly impacted by human interventions in 80 the past, with the aim of acquiring agricultural land. This has resulted in changes to the Vipava river channel's hydromorphological characteristics through river engineering works, as well land use alterations (Magjar et al., 2016). Frequent flood-related problems are present along the studied section in the lower Vipava river valley due to the complex interplay of the catchment's hydrological and topographic characteristics, as well as land use patterns in the floodplain areas. Major flood events with return periods (RP) ranging from 20- to 100-year occurred in 1998, 2009, 2010, and 2012. During the 85 flood of September 2010, with the highest discharge ever measured at the lowest water station Miren (437 m³/s), the towns of Renče and Miren, which are the most exposed to the flood hazard in the study area, were completely cut off from the valley.



The water levels exceeded those of the previous flooding in April 2009, which was classified as a 100-year flood event. In recent decades, flood-related issues have worsened due to the expansion of built-up areas in floodplains and changes in hydraulic conditions in the Vipava river channel. This is mainly caused by the intensive successive overgrowth of the river channel by riparian vegetation. Structural flood protection measures were generally implemented at a local level, addressing specific community needs. The overall effectiveness of these interventions remains highly constrained.

2.2 Methodological framework

The methodology for exploring the uncertainty and sensitivity aspects in flood hazard mapping is presented in Figure 2. The framework was structured into three phases: (1) data acquisition; (2) hydrodynamic model setup with the incorporation of uncertainty and sensitivity analysis; and (3) inundated area extension and flood hazard mapping analysis based on the hydrodynamic model results (inundation depths and flow velocities).

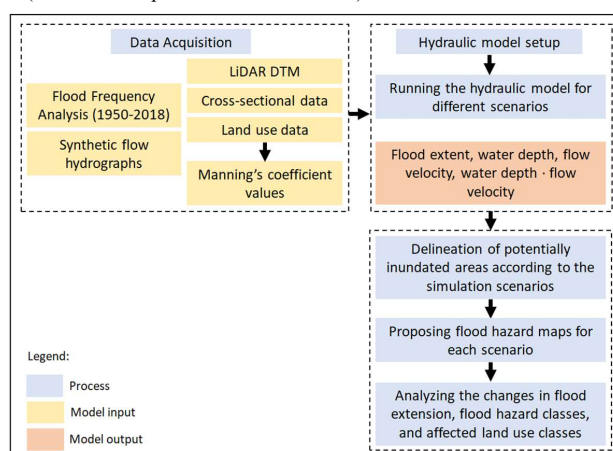


Figure 2: Methodological flowchart.

2.2.1 Overview of the input data

The data were obtained from various governmental entities in the Republic of Slovenia, Table 1 provides a summary of the basic information for the datasets. To simulate flood propagation over the floodplain area, a high-resolution digital elevation model (DTM) based on LIDAR scanning data was utilized. River channel cross-section data were obtained through classical geodetic survey. The hydrological data were summarized following flood frequency analyses (FFA) for the water stations in the studied river section operated by the Slovenian Environmental Agency (ARSO) and previous hydrological studies. Hydraulic simulations utilized a 48-hour SCS dimensionless hydrograph. In general, the characteristics of the 48-hour SCS hydrograph approximate well the Vipava river catchment characteristics as evaluated in previous hydrological studies (Anzeljc, 2021). To account for the uncertainty in the FFA, we considered different values of peak discharge (10%, mean



(design) value, and 90% confidence intervals - CI) for the selected 10-, 100- and 500-year RP. These values were obtained from FFA performed by Piry (2020), which analysed annual discharge peaks using by Pearson III, Log-Pearson III, and GEV distribution. To place the uncertainty in FFA in the context of foreseen climate change, the estimated changes in flood characteristics driven by climate change were summarized from official reports prepared by the Slovenian Environmental Agency (ARSO) on the Climate Change Assessment for Slovenia in the 21st Century (ARSO, 2018). The analysis considered RCP 2.6, RCP 4.5, and RCP 8.5 scenarios following the IPCC guidelines. The flood peaks for the Vipava river are generally expected to rise by 5% (RCP 2.6 scenario), 10% (4.5 RCP scenario) and 20% (8.5 RCP) scenario for the modelled 30-year time horizons (2011–2040, 2041–2070, and 2071–2100) compared to the reference period of 1981–2010.

Table 1: Overview of the dataset used in the study (MNVP - Ministry of Natural Resources and Spatial Planning; GURS - Surveying and Mapping Authority; DRSV - Slovenian Water Agency; MKGP - Ministry of Agriculture, Forestry and Food).

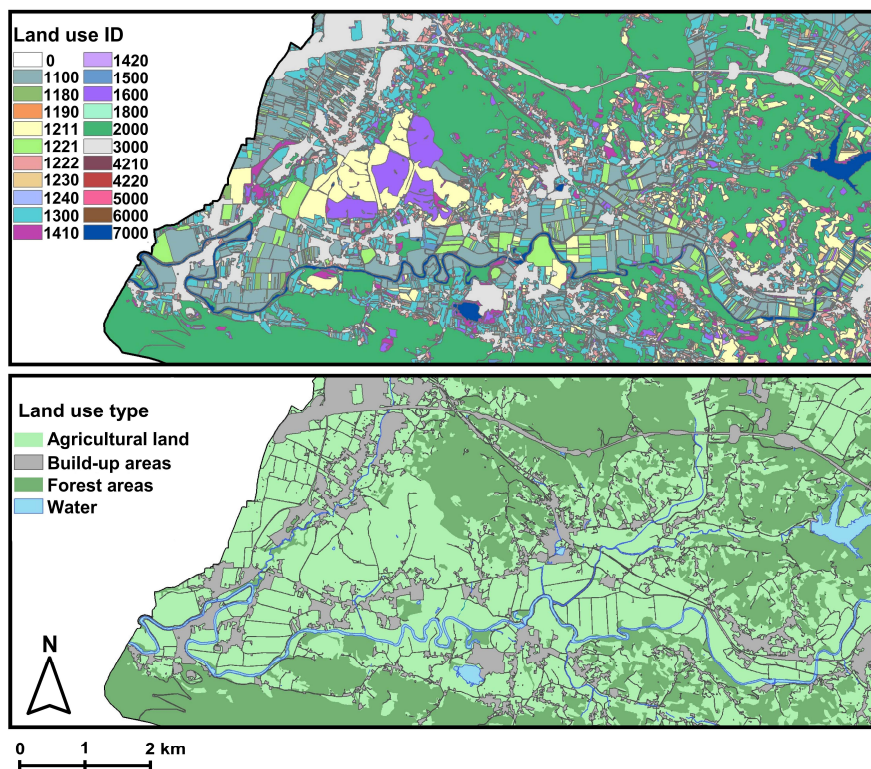
Dataset	Data type	Resolution / Scale	Source
LiDAR DTM	Raster	1m / 5m	MNVP
Orthophoto	Raster	0.25 m	GURS
Cross-sectional data	Vector	/	DRSV
Land use shapefile	Vector	1: 5,000	MKGP
Flood Frequency Analysis	Hydrological	Daily	(Piry, 2020)
River channel and floodplain Manning's roughness coefficients	Hydraulic	/	(NOAA, 2016; USACE, 2022a; NRCS, 2016)

To investigate the impact of hydraulic roughness characteristics of various land use classes in the floodplain areas on the flood extension and other inundation characteristics, detailed land use data (1 m spatial resolution, 21 land use classes) were included in the hydraulic modelling. For each land use class, we considered the range and recommended value of Manning's roughness and the percent impervious value were taken from the literature (NOAA, 2016; USACE, 2022a; NRCS, 2016). The Manning roughness coefficients are listed in Table 2. In the study area, there are various agricultural land uses that do not significantly differ in terms of hydraulic roughness. Therefore, different land use classes may have similar Manning's roughness values, as reported in the literature. The land use in the study areas is highly fragmented as shown in Figure 3 (upper map). Figure 3 (lower map) illustrates the reclassified land use classes, which can be clustered into four characteristic land use categories. The majority of the investigated area is covered by forest (44%), primarily on the hillsides surrounding the lowland, flat areas in the Vipava river valley. Agricultural land covers 43% of the area, mostly in the low-lying area along the river and its tributaries. The built-up areas, which constitute approximately 11% of the total area, are less dominant and highly spatially dispersed.



Table 2: Manning's coefficients for selected floodplain land use classes (MKGP, 2006; NOAA, 2016; USACE, 2022b; USDA, 2016).

Land use ID	Land use type	Manning's n range	Recommended Manning's n
1100	Field or garden	0.02 – 0.05	0.05
1180	Perennial plants in arable land	0.02 – 0.05	0.05
1211	Vineyard	0.07 – 0.16	0.08
1222	Extensive orchard	0.07 – 0.16	0.08
1240	Other perennial crops	0.02 – 0.05	0.05
1300	Permanent grassland	0.025 – 0.05	0.04
1410	Overgrown land	0.025 – 0.05	0.04
1420	Forest tree plantation	0.08 – 0.20	0.12
1500	Trees and shrubs	0.07 – 0.16	0.08
1600	Uncultivated agricultural land	0.025 – 0.05	0.045
1800	Agricultural land overgrown with forest	0.08 – 0.20	0.12
2000	Forest	0.08 – 0.20	0.12
3000	Built-up and related land	0.06 – 0.20	0.12
4220	Other marshy lands	0.05 – 0.085	0.06
5000	Dry open land with special vegetation cover	0.023 – 0.03	0.03
6000	Open land without or with insignificant vegetation cover	0.023 – 0.03	0.03



135 **Figure 3:** (upper map) – Fragmented land use in the study area (land use codes for the main land use classes: forest: land use ID 2000, built-up areas: land use ID 3000, water bodies: land use class 7000, different agricultural land uses: land use IDs 1000-1800); (lower map) – Clustered land use classes.

2.2.2 Hydrodynamic model setup

140 The data presented in the previous section were used in hydrodynamic modelling to run the flood simulations and derive the flood inundation and hazard maps. A combined 1D/2D unsteady flow simulation was performed using the HEC-RAS 6.5 hydrodynamic model. The 1D/2D approach considers lateral interactions between the river channel (1D) and the floodplain (2D), allowing for a more detailed and accurate representation of flood characteristics (Pasquier et al., 2019). The Manning's roughness coefficient values for the Vipava river channel were calibrated against observed water levels during past flood

145 events (Donevska, 2022). The 1D numerical solution was obtained using the Finite Difference method, while the 2D



computational domain was solved using the Diffusion Wave equation (USACE, 2022a). Different 2D grid cell sizes (5 - 100 m) were tested, smaller grid cell sizes considerably prolonged the simulation times. A 20 m cell size was identified as optimal in view of impact of 2D grid cell resolution on the difference in the modelled water level elevations and the inundated area extension. To ensure simulation stability and minimize percent error (USACE, 2022b), an adjustable time step based on the Courant number (0.45-1) was employed. Unchanged numerical settings were used for all simulation runs (Donevska, 2022). The hydrodynamic model calibration was achieved through the adjustment of the river channel and floodplain roughness coefficients to align the modelled flood extension and water levels with the observed ones. The hydrodynamic model validation, based on few flood events with available data on water levels at specific locations and inundation extent at specific subsections along the Vipava river study area, demonstrated a satisfactory agreement with the observed data. The mean difference between the modelled and observed inundated area extension at selected river subsections was 6% (standard deviation of 3%), which could be regarded as a general indicator of the uncertainty in the extent of the modelled inundation areas.

Conducting numerous simulations on extensive river segments may not be feasible for routine use, as hydrodynamic models typically demand substantial computational time. In this instance, each simulation with the selected model parameters required approximately 3 to 5 hours to complete. However, these simulations are necessary for conducting uncertainty and sensitivity analysis of simulation results. To tackle the challenge posed by numerous simulations runs, we focused on targeted boundary scenario ensembles to evaluate the influence of model input data and parameters. These factors were generally identified in literature as critical for flood hazard assessment (e.g., McCarthy et al., 2014; Annis et al., 2020). The selected scenario ensembles aimed to consider the boundary conditions in terms of hydrological and hydraulic input data, such as the worst (e.g. by considering upper limits of the peak discharge confidence intervals and high roughness coefficients values) and the best-case scenarios (lower limits of the peak discharge confidence intervals and low values of roughness coefficients). Accordingly, three groups of scenario ensembles were defined to consider the following aspects. Scenario ensemble S1 addresses the impact of hydrological uncertainty associated with FFA for assessing discharge peaks. 10% and 90% confidence intervals and the design peak discharge values were considered. Scenario ensemble S2 examines the sensitivity of simulation results to ranges of floodplain hydraulic roughness coefficients. Scenario ensemble S3 focuses on the impact of hydraulic roughness of the Vipava river channel. The calibrated Manning coefficient for the Vipava river channel (roughness coefficient values ranging from 0.04 to 0.08) based on past flood events (scenario S3II), was compared to the designed roughness coefficient of 0.035 (scenario S3I), which was determined during the river regulation works in the 1970s. Table 3 lists the 8 examined scenarios.

Table 3: Uncertainty/sensitivity analysis scenario ensembles.

Scenario ensemble	Uncertainty parameter	Scenario	Varying model input
S1	Peak discharge	I	10% confidence interval
		II	Design peak discharge value
		III	90% confidence interval



S2	Floodplain Manning's roughness coefficients	I	Minimum floodplain Manning's values
		II	Recommended floodplain Manning's values
		III	Maximum floodplain Manning's values
S3	Channel Manning's roughness coefficients	I	Designed channel Manning's value = 0.035
		II	Calibrated channel Manning's values

175

The flood hazard maps were elaborated in accordance with the national legislation of the Republic of Slovenia, which considers flood peaks with RP of 10, 100, and 500 years. The flood hazard classes were defined based on the combination of flood peak RP, water depth and the flow depth-velocity product, which are the most common criteria used for mapping flood hazard in many EU countries (Polese et al., 2024). The flood hazard classes criteria that were considered in the analysis are summarized in Table 4. The flood hazard maps were prepared by exporting water depth and the depth-velocity product raster data to GIS software to prepare the flood hazard maps. The most relevant criteria for defining spatial extension of flood hazard classes for the scenario ensembles was the inundation depth. According to the flood hazard class criteria, the depth-velocity product was the prevailing flood hazard criteria only in spatially constrained areas along the main Vipava river channel where channel banks or levees were intensively overtopped during specific flood scenario.

185

Table 4: Flood hazard class criteria.

Flood hazard class	Criteria
High	At discharge Q_{100} or water level G_{100} , water depth $\geq 1.5\text{m}$ or water depth \cdot water velocity $\geq 1.5\text{m}^2/\text{s}$
Medium	At discharge Q_{100} or water level G_{100} , $1.5\text{m} >$ water depth $\geq 0.5\text{m}$ OR $1.5\text{m}^2/\text{s} >$ water depth \cdot water velocity $\geq 0.5\text{m}^2/\text{s}$ or where at discharge Q_{10} or water level G_{10} , water depth $> 0\text{m}$.
Low	At discharge Q_{100} or water level G_{100} , water depth $< 0.5\text{m}$ OR water depth \cdot water velocity $< 0.5\text{m}^2/\text{s}$
Other	At discharge Q_{500} water depth $\geq 0\text{m}$ or where flooding could occur due to extraordinary natural or human-induced events

2.2.3 Global sensitivity analysis and probability of inundation

Global sensitivity analysis of the hydrodynamic simulation results was conducted using the Morris method, a computationally efficient screening approach that perturbs one parameter at a time along randomized trajectories in the parameter space and evaluates resulting changes in model output (Herman et al., 2013; Nabi et al., 2021). The method produces two diagnostic indices: the mean absolute elementary effect (μ^*), indicating overall importance, and the standard deviation of effects (σ), indicating nonlinear behaviour or interactions. Because the Morris method demands fewer model simulations than variance-based approaches, it is an attractive choice for hydrologic and hydrodynamic modelling when computational resources are limited but dependable parameter sensitivity analysis is required (Li et al., 2023). This efficiency makes the Morris method

195



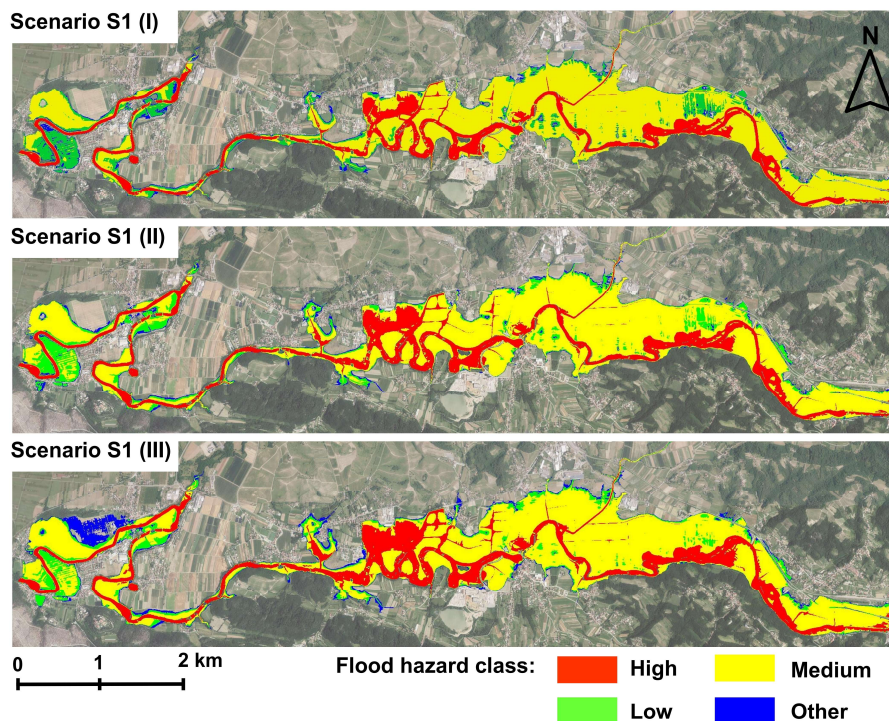
particularly valuable in flood-risk mapping workflows, where uncertainties in hydrodynamic model input data and sensitivity of the models strongly influence inundation patterns (Rebolho et al., 2018).

Assessing inundation probabilities offers valuable insight into the likelihood and spatial distribution of flood events, enabling a more nuanced understanding of flood risk (Merz et al., 2014). The weighted exceedance probability of inundation was
200 calculated by combining binary inundation outcomes from multiple hydraulic model simulations using RP based weights. For each simulation, inundation depth raster was used to derive a binary indicator of flooding (using threshold of 0.01 m water depth), which was then weighted by the annual exceedance probability. The weighted exceedance probability at each grid cell was obtained as the normalized weighted mean of the binary indicators, thereby emphasizing more frequent events (e.g., Q_{10}) relative to rarer extremes (e.g., Q_{500}). By aggregating inundated areas detected within the scenario ensembles in a
205 probabilistically consistent manner, we obtain comprehensive information on inundation probabilities covering the considered flood RP.

3 Results and Discussion

3.1 Uncertainty in hydrological input data

Uncertainty in the magnitude of the design discharge peak is generally a statistical issue that requires the selection of a specific
210 probability distribution in the FFA. In our case, the impact of the uncertainty in the estimation of the peak discharge (considered through the 10% and 90% confidence intervals of the FFA) expresses considerable influence on the simulation results of the hydrodynamic model. Comparing the results associated with the 10% confidence interval value and the design discharge peak value, the increase in the flood inundation area is 5-6%, while the difference in the flood extent between the design discharge value and the 90% confidence interval value is in the range 4-7%. The difference in the flood extent between the 10% and the
215 90% confidence interval values is 11%, 9%, and 12% for 10-, 100-, and 500-year RP, respectively. This is further reflected in the spatial distribution of the flood hazard classes (Figure 4).



220 **Figure 4: Flood hazard class spatial extension for scenario ensemble S1 - uncertainty in peak discharge estimation. (upper map): 10% confidence interval; (middle map): design discharge peak value; (lower map): 90% confidence interval. Imagery sources: GURS, Esri, Google Earth © 2025.**

The increase in the total flood-prone area caused changes in the spatial extent of the high flood hazard class (an increase of approx. 30%) when comparing the 10% and 90% confidence interval discharge values (Figure 5). The area of the medium flood hazard class also increases slightly, while the area of the low hazard class decreases at the expense of the higher hazard classes expansion. The spatial expansion of the other flood hazard class significantly increases with the peak discharge (60% when comparing the design discharge and the 90% confidence interval values), visually evident mainly along the right bank in the downstream part of the studied Vipava river section where the floodplain is relatively flat (Figure 4). This area is mostly used for intensive agriculture (orchards), in smaller parts also urbanized.

225

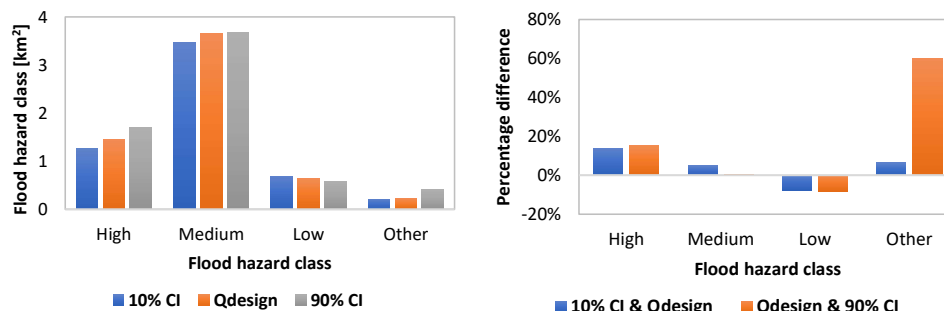


Figure 5: Comparison of the spatial extension of flood hazard classes for scenario ensemble S1 – uncertainty in peak discharge estimation.

230 There is no guarantee that any of the statistical methods will always produce design discharges that will match the observed flood peak values. Moreover, determining the design discharge for a given RP may be subjected to additional uncertainties related to the non-stationarity of the discharge data and the resulting impact on the analysis of flood magnitude and frequency (Machado et al., 2015; Stephens & Bledsoe, 2020). Interestingly, the considered confidence intervals of the FFA are in the ranges of the anticipated peak discharge increase for the RCP 2.6 and 4.5 scenario according to the assessment of climate

235 change in Slovenia until the end of the 21st century (ARSO, 2018). The worst-case RCP 8.5 scenario (anticipated 20% increase in flood peaks) somewhat exceeds the 90% FFA confidence intervals for all considered flood peak RP. Therefore, the uncertainty in the FFA could be effectively used also to account the potential impact of selected climate change on the flood peaks according to the RCP 2.6 and 4.5 scenarios. This demonstrates a direct link between hydrological uncertainty in FFA and the projected rise in peak discharges driven by climate change, suggesting that integrating both aspects within flood

240 modelling could offer a more comprehensive approach to anticipated future flood hazards.

3.2 Sensitivity of the flood hazard mapping on the hydraulic roughness characteristics

The problem of selecting the appropriate hydraulic roughness coefficient for the floodplains considered as the 2D

245 computational domain in the hydrodynamic model simulations has been discussed by several authors (e.g., Casas et al, 2010; Wright et al., 2017; Zahidi et al., 2018). The sensitivity analysis of the varying floodplain Manning’s roughness coefficients of the particular land use patterns in the studied floodplain areas overall expresses increase in the inundation extent. The impact of higher roughness coefficients in the floodplains on inundation extent is well-documented in hydraulic modelling literature, where higher roughness values typically associated with vegetated or urbanized floodplains lead to slower flow velocities and

250 increased water surface elevations, thereby expanding the inundation area. Warmink et al. (2013) quantified the uncertainty in



design water levels due to hydraulic roughness in the River Waal, showing that vegetation roughness in floodplains contributed significantly to the overall uncertainty. Praskiewicz et al. (2020) demonstrated that flood extent predictions are highly sensitive to both topographic resolution and Manning's n values, especially in floodplains where land cover is variable. The selection of the higher floodplain roughness conditions could effectively account for the future changes in floodplain land use on the inundation extent. However, the results indicate that the Manning's roughness coefficients of the floodplain areas have a relatively limited influence on the flood extent from the spatial perspective of the analysed Vipava river section. The difference in the inundation extent when comparing the scenarios of minimum and maximum Manning's values is about 6% for the 10-year RP flood and around 4% for the 100- and 500-year RP floods. The variability in the extension of the inundated areas and consequent extension of flood hazard areas is more noticeable in the areas with gentle slopes, mostly along the right bank of the Vipava river channel, where the floodplains are wider (Figure 6).

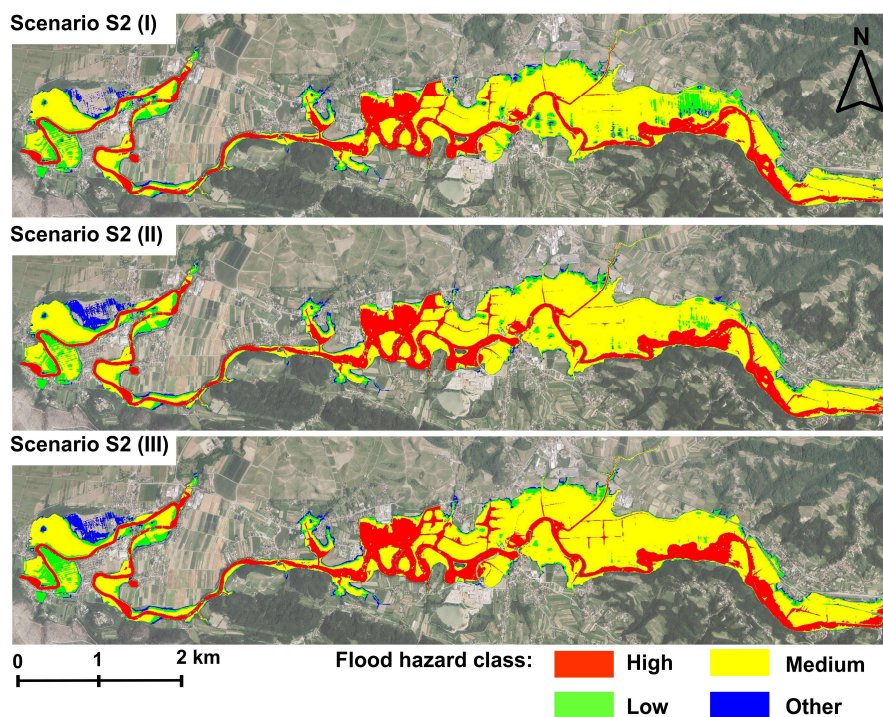


Figure 6: Flood hazard class spatial extension for scenario ensemble S2 - different floodplain roughness characteristics. (upper map): low floodplain roughness; (middle map): recommended floodplain roughness; (lower map): high floodplain roughness. Imagery sources: GURS, Esri, Google Earth © 2025.



265 One should note that the difference in inundation extend of few % is generally in the range of the uncertainty of the simulated
 inundation areas extension. In this respect, the influence of varying floodplain roughness coefficient appears to be limited.
 However, some interesting shifts in the flood hazard class extension could be observed. The highest variability in the spatial
 extent was observed for the low flood hazard class, which amounted to a total decrease in the spatial extent for approx. 25%
 when comparing the scenarios of minimum and maximum roughness coefficients of the floodplain areas (Figure 7). Some
 270 parts of the flood inundation area that were assigned to the lower hazard class when considering lower Manning’s coefficient
 values were assigned to the higher hazard class when considering increased Manning’s coefficient values.

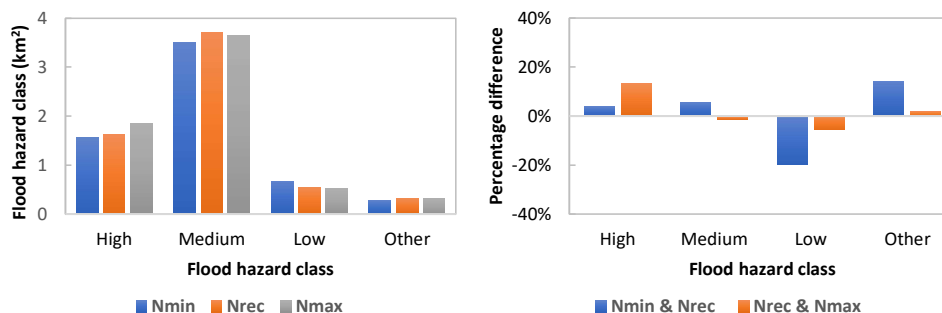
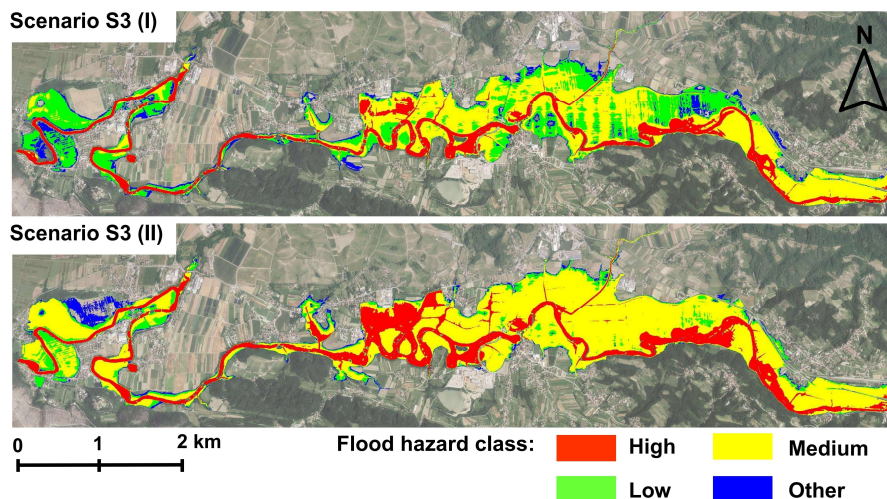


Figure 7: Comparison of the spatial extension of flood hazard classes for scenario ensemble S2 – different floodplain roughness characteristics.

When several sections of the Vipava river channel were regulated and widened in the 1970s and 1980s, the designed Manning’s
 275 values of the river channel were in the range of 0.030 to 0.035 and the designed hydraulic conveyance was in the range of 10
 to 20-year flood RP. However, in recent decades, the channel cross-section has been successively heavily overgrown by the
 riparian vegetation, and recent flood events have shown a significant increase in the channel area hydraulic roughness. The
 inundation and flood hazard classes extension obtained from the simulation using the designed channel Manning’s coefficient
 value and the calibrated values based on past flood events were compared. A significant increase in the flood inundation area
 280 for a 10-year RP flood could be detected demonstrating a high sensitivity of simulated inundation area expansion to channel
 roughness coefficients. Higher main channel roughness coefficients significantly reduce the hydraulic conductivity of the
 Vipava River channel, causing the flow to overtop the channel banks intensively even during peak flows with a lower RP (e.g.,
 Q_{10}). Changes in the channel roughness coefficient causes a considerable increase in the inundation extent and spatial extent
 of higher flood hazard classes (Figure 8). When comparing the simulation results associated with the designed and the
 285 calibrated channel Manning’s roughness coefficients (the values close to maximum recommended), the overall increase in the
 inundated area was approx. 45% for a 10-year flood RP. For 100- and 500-year RP events, the increase in the flood extent was
 15% and 11%, respectively.



290 **Figure 8: Simulation results for scenario ensemble S3 - different river channel roughness characteristics. (upper map): design channel roughness; (lower map): calibrated channel roughness. Imagery source: GURS, Esri, Google Earth © 2025.**

The spatial extent of the high and medium flood hazard classes shows an increase of approx. 40%, while the low and other flood hazard classes show a decrease of approx. 90% and 40%, respectively (Figure 9). It should be noted that the expansion of the higher flood hazard classes causes a decrease in the expansion of inundated areas previously classified in the low and other flood hazard classes. Slater (2016) studied impact of changes in river channel hydraulic capacity on flood hazard trends in England and Wales. His results showed that changes in the channel capacity would result in considerable changes in the flood frequency. Our results suggest that overlooking the potential influence of changes in channel roughness may be extremely dangerous, especially with respect to more frequent flood events. Sensitivity testing of hydrodynamic simulation workflows, especially related to the succession changes in river channel roughness, can greatly enhance the robustness of flood hazard assessment. Changes in spatial expansion of high/medium flood hazard class, which in many countries poses considerable restrictions for the spatial planning, should be effectively incorporated in flood risk mitigation strategies as discussed by Greiving et al. (2025) and Bodoque et al. (2023).

295

300

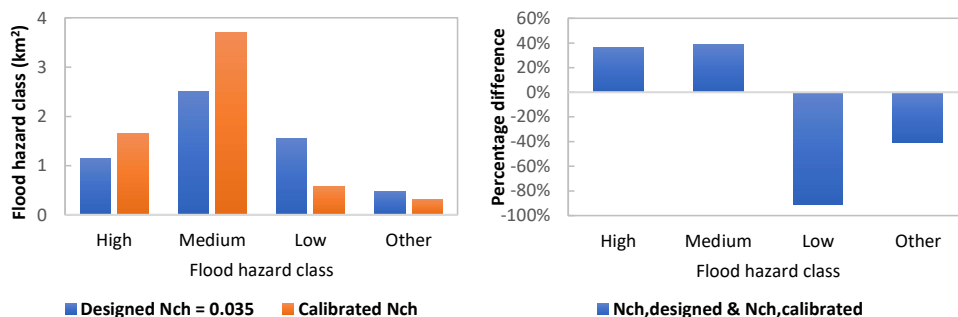


Figure 9: Comparison of the spatial extension of flood hazard classes for scenario ensemble S3 – different river channel roughness characteristics.

305

3.3 Sensitivity analysis of inundation extent and maximum inundation depths

The observed changes in spatial extension of inundated areas appears to be conditioned especially by the specific topography of the area, FFA uncertainty and also roughness characteristics of the Vipava river channel. The topography of the floodplain affects the extension of the inundated areas for different RP, as it limits the increase in inundated area extent in some parts of the floodplains. The differences in the spatial extent of the inundated areas are smaller in the narrower parts of the floodplain. On the contrary, the wider floodplain sections extending along the right bank show more pronounced spatial variability of flood extent and hazard classes.

The results of the Morris method sensitivity analysis for inundation extent and maximum inundation depth are shown in Figure 10. The results indicate that the inundation area is primarily controlled by variations in channel roughness and peak discharge, which exhibited the largest μ^* values and thus the strongest main effects. In contrast, floodplain roughness contributed only marginally to variations in inundation extent, indicating that spatial expansion of flooding is relatively insensitive to floodplain roughness characteristics. For maximum inundation depth, peak discharge emerged as the dominant driver, while channel roughness showed a secondary but appreciable influence. Across all outputs, σ values were low, suggesting largely linear responses with minimal parameter interactions within the considered scenario ensembles. Overall, these results indicate that both, uncertainty in peak discharge estimate and sensitivity to channel roughness, should be prioritized in hydrodynamic simulation and scenario ensembles selection for flood hazard mapping.

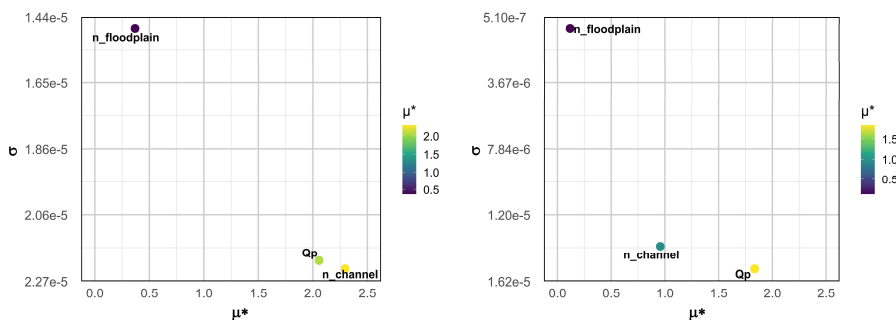


Figure 10: Results of the Morris method sensitivity analysis for inundation extent (left) and maximum inundation depth (right).

325 3.4 Probability of inundation in view of the critical land use classes

The main purpose of flood hazard maps elaboration is to steer the future spatial planning and restrict the unwise (e.g. build-up or intensive agriculture) land use in areas potentially exposed to flood hazard. In the three analysed scenario ensembles, the area of potentially inundated agricultural land ranges from 2.35 km² to 4.94 km². The flood-prone built-up areas only cover a small portion of the inundated areas (0.06-0.25 km²). Due to the high spatial fragmentation, only a few larger built-up areas

330 (Figure 1) have high flood risk. The differences in the affected agricultural land use areas lies in the ranges up to 55% for a 10-year flood, up to 20% for a 100-year flood, and up to 15% for a 500-year RP flood event. The difference in the extent of inundated built-up areas ranges up to 70% for a 10-year flood event and up to 50% for 100- and 500-year RP events, respectively. Figure 11 shows a map of weighted exceedance probability of inundation. By identifying areas that are repeatedly

335 inundated across the considered scenario ensembles (elevated probability of inundation, e.g. > 0.5), consideration of inundation probability could support the precautionary principle, whereby land-use decisions are informed by the potential inundation probability conditioned by uncertain future conditions. Probabilistic flood hazard mapping has been shown to reveal spatial patterns of hidden or transitional risk that are not captured by deterministic flood boundaries, making it particularly suitable for risk zoning and development control in flood-prone areas (Stephens and Bledsoe, 2020). Consequently, inundation exceedance probability maps offer a robust evidence base to support spatial planning policies aimed at restricting or avoiding

340 future development in areas with persistent or uncertain flood hazard.

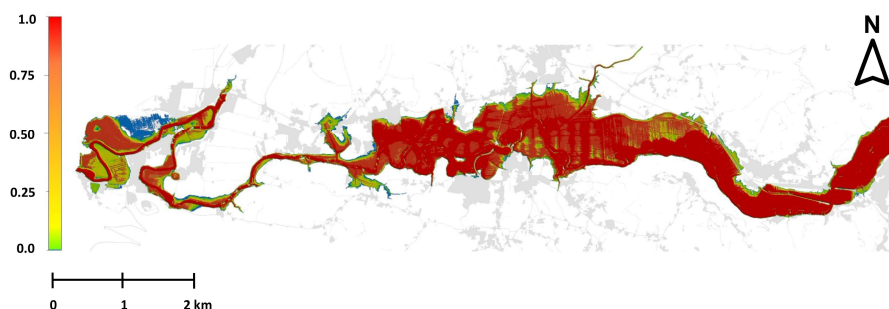


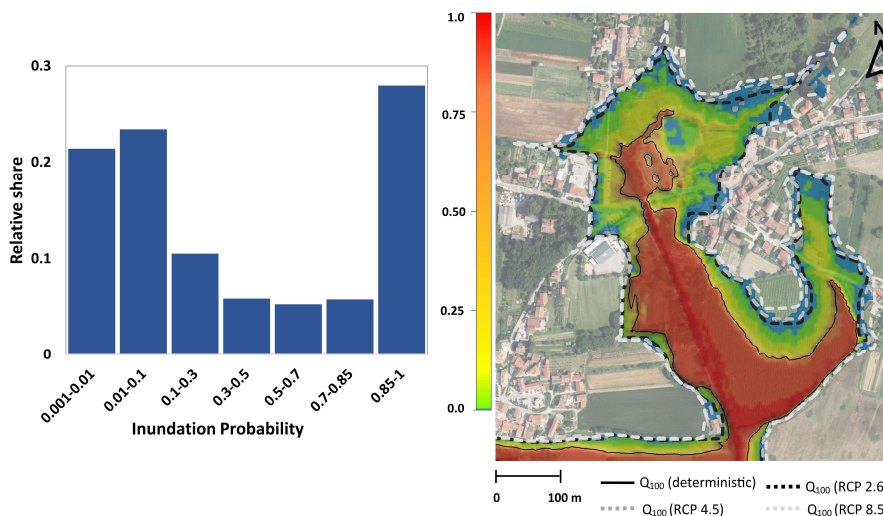
Figure 11: Weighted exceedance probability of inundation for the considered scenario ensembles. Gray shaded polygons indicate build-up areas.

345 Figure 12 (left) shows inundation probability over built-up areas expressed as relative shares of inundated areas. Interestingly, approx. 40% of the build-up areas are positioned in areas of elevated inundation probability (> 0.5) according to the considered scenario ensembles. It would be highly advisable to avoid future intensive development in such areas under uncertain future flood conditions. Large proportion of build-up areas falling into high inundation probability bin (> 0.85) is related to road infrastructure crossing the floodplain areas. Road failures induced by floods propagate far beyond inundated segments through

350 network bottlenecks and interdependencies, highlighting the need for integrated flood hazard assessments for transport systems. Mapping inundation probability could be found crucial to identify the most vulnerable sections of critical road infrastructure, enabling targeted mitigation and protection measures against flood hazards.

Figure 12 (right) shows the weighted exceedance probability of inundation and the deterministic inundation extent of the Q_{100} RP design flood event as regulatory flood hazard boundary. Additionally, inundation extents of the Q_{100} RP design flood event for RCP 2.6, RCP 4.5 and RCP 8.5 scenarios are also shown. One can see that weighted inundation probability derived from the considered scenario ensembles encloses also most of the foreseen climate change scenarios, the only exception being the worst-case RCP 8.5 scenario which generally exceeds the inundation extent of the considered scenario ensembles. Factoring in hydrological uncertainty with climate change may reveal greater changes in flood patterns, with future flood hazard zones extending beyond current regulatory boundaries. Sharing these insights with probability maps could considerably improve

360 understanding of uncertainty and sensitivity in flood hazard classification, particularly regarding potential climate change impacts.



365 **Figure 12: (left) Weighted inundation probabilities over built-up areas expressed as relative shares of inundated build-up areas. (Right) Comparison of weighted inundation probability, the deterministic inundation extent of the Q_{100} RP design flood event and inundation extent for RCP 2.6, RCP 4.5 and RCP 8.5 scenarios. Imagery source: GURS.**

The results shown in Figure 12 clearly demonstrate that spatial development near “deterministic” flood hazard boundaries combined with potential compounding impacts of changed hydraulic conditions in the river channel, uncertainty related to the FFA or anticipated changes in flood peaks due to climate change, have a high potential to considerably increase the flood risk of built-up areas. Stephens & Bledsoe (2023) show that flood hazard maps that do not account for uncertainty may substantially underestimate exposure to future flooding and provide a false sense of protection. Their findings support the need for robust decision-making in flood risk management to cover a range of possible alternative model outcomes that could be provided by our approach. This can help adapting the land use planning in areas that are potentially exposed to flood hazards and also strengthen the decision support systems as suggested by Van der Most et al. (2018). Our results show that uncertainty and sensitivity in flood hazard mapping are not merely theoretical issues; they have practical consequences for spatial planning and risk mitigation in topographically complex landscapes with highly dispersed land use, such as the studied Vipava River section.

4. Conclusions

380 Due to the numerous sources of uncertainty in hydrological input data and the sensitivity of hydrodynamic modelling results to input parameters, various questions about reliability and validity inevitably arise during flood hazard assessment. Our study aimed to systematically address and quantify hydrological uncertainty and the sensitivity of hydrodynamic simulations, as well



as highlight the evident lack of information when depicting flood hazards as only discrete boundaries. The proposed approach considers possible deterioration of the flood hazard situation, e.g., due to successional hydraulic roughness changes or climate change impacts on floods, by considering the FFA confidence intervals. The analyzed scenario ensembles demonstrate that the extension of inundated areas is significantly sensitive to channel roughness, especially for more frequent floods. Any alterations to the river channel that affect its hydraulic roughness must be thoroughly evaluated and included in flood hazard assessments. Uncertainty analysis could be expanded by generating additional uncertain model inputs/parameters and performing multiple simulation runs (e.g., by considering additional scenario ensembles), which could provide more detailed inundation probability information for specific areas. However, performing such an analysis requires considerable computational time. Nevertheless, we believe that the results obtained by analyzing limited “boundary” scenario ensembles are adequate for quantifying the sensitivity of inundation extent and identifying sources of uncertainty affecting flood inundation and hazard maps.

Our approach highlights the importance of incorporating uncertainty and sensitivity analyses into standard flood hazard mapping practices. This integration is crucial for safeguarding vulnerable land uses and critical infrastructure against the evolving challenges posed by climate change. These results could improve the communication of the uncertainty and sensitivity aspects of flood hazard mapping to stakeholders involved in spatial planning. This could provide a more nuanced understanding of potential changes in flood hazard, supporting proactive and adaptive management strategies tailored to fragmented land use contexts.

Code/Data availability

The datasets used in the study are freely available. The hydrodynamic modelling results used in this study are publicly available from the Zenodo repository at: [10.5281/zenodo.20135245](https://zenodo.org/doi/10.5281/zenodo.20135245).

Author contributions

SR and MM conceptualized the methodology; JD built the hydrodynamic model and performed the simulations. SR and JD write the original manuscript. MM acquired funding and conducted project administration. SR validated the simulation results, SR and MM supervised the research.

Competing interests

The authors declare that they have no conflict of interest.

Acknowledgements

We would like to express our sincere gratitude to the reviewers for their constructive comments.



410 **Financial support**

The study was carried out in the scope of the Erasmus Mundus Flood Risk Management master program (Grant of the first author) and the UNESCO Chair on Water-related Disaster Risk Reduction activities. Financial support was provided by the University of Ljubljana Development Fund, Slovenian target project V2-2371, Slovenian national core funding No. P2-0180 co-financed by the Slovenian Research and Innovation Agency, Slovenian Ministry of Education, Science and Sport under

415 UNESCO's Intergovernmental Hydrological Programme and Slovenian Ministry of Natural Resources and Spatial Planning.

References

Alfonso, L., Mukolwe, M., and Di Baldassarre, G.: Probabilistic Flood Maps to support decision-making: Mapping the Value of Information, *Water Resour. Res.*, 52(2), 1026-1043, doi:10.1002/2015wr017378, 2016

420 Annis, A., Nardi, F., Volpi, E., and Fiori, A.: Quantifying the relative impact of hydrological and hydraulic modelling parameterizations on uncertainty of inundation maps, *Hydrol. Sci. J.*, 65(4), 507–523, <https://doi.org/10.1080/02626667.2019.1709640>, 2020

Anzeljč, D.: Hydrological study of the Vipava river catchment. Ministry for the Environment and Spatial Planning of the Republic of Slovenia (in Slovenian), 2021

425 ARSO: Assessment of climate change in Slovenia until the end of the 21st century. Environmental Agency of the Republic of Slovenia (in Slovenian), 152 pp, 2018

Bates, P.: Flood Inundation Prediction, *Ann. Rev. Fluid Mech.*, 54, 287-315, <https://doi.org/10.1146/annurev-fluid-030121-113138>, 2022

Bodoque, J. M., Esteban-Muñoz, Á., and Ballesteros-Cánovas, J. A.: Overlooking probabilistic mapping renders urban flood risk management inequitable, *Commun. Earth Environ.*, 4(940). <https://doi.org/10.1038/s43247-023-00940-0>, 2023

430 Casas, A., Lane, S.N., Yu, D., and Benito, G. A.: method of parameterising roughness and topographic sub-grid scale effects in hydraulic modelling from LiDAR data, *Hydrol. Earth Syst. Sci.*, 14(8), 1567–1579, <https://doi.org/10.5194/hess-14-1567-2010>, 2010

435 Donevska, J.: Analysis of uncertainties in the process of flood hazard maps elaboration, MSc thesis, University of Ljubljana, Faculty of Civil and Geodetic Engineering, Ljubljana, <https://repositorij.uni-lj.si/lzpisGradiva.php?id=141740&lang=slv>, 2022

Glas, H., Deruyter, G., De Maeyer, P., Mandal, A., and James-Williamson, S.: Analyzing the sensitivity of a flood risk assessment model towards its input data, *Nat. Hazards Earth Syst. Sci.*, 16, 2529-2542, <https://doi.org/10.5194/nhess-16-2529-2016>, 2016

440 Greiving, S., Wolf, S., Michalski, D., and Fleischhauer, M.: Flood Risk Mitigation by Spatial Planning—Lessons Learned From Municipal Consultation, *J. Flood Risk Manag.*, 18(2), e70066, <https://doi.org/10.1111/jfr3.70066>, 2025



- Hashimoto, M., Kawaike, K., Deguchi, T., Haque, S., Paul, A., Salehin, M., and Nakagawa, H.: Multi-scale flooding hazards evaluation using a nested flood simulation model: case study of Jamuna River, Bangladesh, *Int. J. River Basin Manag.*, 21(2), 167–179, <https://doi.org/10.1080/15715124.2021.1935977>, 2023
- Herman, J. D., Kollat, J. B., Reed, P. M., and Wagener, T.: Method of Morris effectively reduces the computational demands of global sensitivity analysis for distributed watershed models, *Hydrol. Earth Syst. Sci.*, 17(7), 2893-2903, <https://doi.org/10.5194/hess-17-2893-2013>, 2013
- Herrera, P. A., Marazuela, M. A., and Hofmann, T.: Parameter estimation and uncertainty analysis in hydrological modeling, *Wiley Interdiscip. Rev.*, 9(1), e1569. <https://doi.org/10.1002/wat2.1569>, 2022
- Jelovčan, M., Šraj, M.: Comprehensive low-flow analysis of the Vipava river. *Acta Geogr. Slov.*, 62(1), 7–22. <https://doi.org/10.3986/AGS.9399>, 2022.
- Li, D., Ju, Q., Jiang, P., Huang, P., Xu, X., Wang, Q., ... and Zhang, Y.: Sensitivity analysis of hydrological model parameters based on improved Morris method with the double-Latin hypercube sampling, *Hydrol. Res.*, 54(2), 220-232, <https://doi.org/10.2166/nh.2023.109>, 2023
- Lim, N. J., Brandt, S. A., and Seipel, S.: Assessment of how uncertainty representation in flood maps can affect geographic-based decisions, *Discover Water*, 4(1), 120. <https://doi.org/10.1007/s43832-024-00170-1>, 2024
- Machado, M. J., Botero, B. A., López, J., Francés, F., Díez-Herrero, A., and Benito, G.: Flood frequency analysis of historical flood data under stationary and non-stationary modelling, *Hydrol. Earth Syst. Sci.*, 19(6), 2561-2576, <https://doi.org/10.5194/hess-19-2561-2015>, 2015
- Magjar, M., Suhadolnik, P., Šantl, S., Vrhovec, Š., Krivograd Klemenčič, A., and Smolar-Žvanut, N.: Vipava River Basin Adaptation Plan. In: BeWater project, 2016
- Maranzoni, A., D'Oria, M., and Rizzo, C.: Quantitative flood hazard assessment methods: A review, *J. Flood Risk Manag.*, 16(1), <https://doi.org/10.1111/jfr3.12855>, 2023
- McCarthy, S., Beven, K., and Leedal, D.: Framework for assessing uncertainty in fluvial flood risk mapping: CIRIA Report No. C721, 2014
- Merz, B., Aerts, J., Arnbjerg-Nielsen, K., Baldi, M., Becker, A., Bichet, A., Blöschl, G., Bouwer, L. M., Brauer, A., Cioffi, F., Delgado, J. M., Gocht, M., Guzzetti, F., Harrigan, S., Hirschboeck, K., Kilsby, C., Kron, W., Kwon, H.-H., Lall, U., Merz, R., Nissen, K., Salvatti, P., Swierczynski, T., Ulbrich, U., Viglione, A., Ward, P. J., Weiler, M., Wilhelm, B., and Nied, M.: Floods and climate: emerging perspectives for flood risk assessment and management, *Nat. Hazards Earth Syst. Sci.*, 14, 1921–1942, <https://doi.org/10.5194/nhess-14-1921-2014>, 2014.
- Mishra, A., Mukherjee, S., Merz, B., Singh, V. P., Wright, D. B., Villarini, G., ... and Stedinger, J. R.: An overview of flood concepts, challenges, and future directions, *J. Hydrol. Eng.*, 27(6), 03122001. [https://doi.org/10.1061/\(ASCE\)HE.1943-5584.0002164](https://doi.org/10.1061/(ASCE)HE.1943-5584.0002164), 2022



- Nabi, S., Ahanger, M. A., and Dar, A. Q.: Investigating the potential of Morris algorithm for improving the computational constraints of global sensitivity analysis, *Environ. Sci. Pollut. Res.*, 28(43), 60900-60912, <https://doi.org/10.1007/s11356-021-14994-0>, 2021
- NOAA: Office for Coastal Management. C-CAP Regional Land Cover and Change, <https://coast.noaa.gov/digitalcoast/data/ccapregional.html>, 2016
- Nogherotto, R., Fantini, A., Raffaele, F., Di Sante, F., Dottori, F., Coppola, E., and Giorgi, F. A combined hydrological and hydraulic modelling approach for the flood hazard mapping of the Po river basin, *J. Flood Risk Manag.*, 15(1), <https://doi.org/10.1111/jfr3.12755>, 2022
- NRCS: Manning's n Values for Various Land Covers to Use for Dam Breach Analyses by NRCS in Kansas, <https://rashms.com/wp-content/uploads/2021/01/Mannings-n-values-NLCD-NRCS.pdf>, 2016
- Pasquier, U., He, Y., Hooton, S., Goulden, M., and Hiscock, K. M.: An integrated 1D–2D hydraulic modelling approach to assess the sensitivity of a coastal region to compound flooding hazard under climate change, *Nat. Hazards*, 98(3), 915-937, <https://doi.org/10.1007/s11069-018-3462-1>, 2019
- Paulik, R., Zorn, C., Wotherspoon, L., and Harang, A.: Model parameter influence on probabilistic flood risk analysis, *Int. J. Disaster Risk Reduct.*, 100, 104215. <https://doi.org/10.1016/j.ijdr.2023.104215>, 2024
- Pavesi, L., Volpi, E., and Fiori, A.: Flood risk assessment through large-scale modeling under uncertainty, *Nat. Hazards Earth Syst. Sci.*, 24(12), 4507-4522. <https://doi.org/10.5194/nhess-24-4507-2024>, 2024
- Piry, M.: Analysis of the design discharges by considering the uncertainty, MSc thesis, University of Ljubljana, Faculty of Civil and Geodetic Engineering, Ljubljana, <https://repozitorij.uni-lj.si/Dokument.php?id=138645&lang=slv>, 2020
- Polese, M., Tocchi, G., Babič, A., Dolšek, M., Faravelli, M., Quaroni, D., ... and Prota, A.: Multi-risk assessment in transboundary areas: A framework for harmonized evaluation considering seismic and flood risks, *Int. J. Disaster Risk Reduct.*, 1012024, 104275, <https://doi.org/10.1016/j.ijdr.2024.104275>, 2024
- Praskievicz, S., Carter, S., Dhondia, J., and Follum, M.: Flood-inundation modeling in an operational context: sensitivity to topographic resolution and Manning's n, *J. Hydroinform.*, 22(5), 1338-1350. <https://doi.org/10.2166/hydro.2020.005>, 2020
- Rebolho, C., Andréassian, V., and Le Moine, N.: Inundation mapping based on reach-scale effective geometry, *Hydrol. Earth Syst. Sci.*, 22(11), 5967-5985. <https://doi.org/10.5194/hess-22-5967-2018>, 2018
- Simões, N., Ochoa-Rodríguez, S., Wang, L.-P., Pina, R., Marques, A., Onof, C., and Leitão, J.: Stochastic Urban Pluvial Flood Hazard Maps Based upon a Spatial-Temporal Rainfall Generator, *Water* 7(12), 3396-3406. doi:10.3390/w7073396, 2015
- Slater, L. J.: To what extent have changes in channel capacity contributed to flood hazard trends in England and Wales? *Earth Surf. Process. Landf.*, 41(8), 1115-1128, <https://doi.org/10.1002/esp.3927>, 2016
- Smart, G. M.: Improving flood hazard prediction models, *Int. J. River Basin Manag.*, 16(4), 449-456, <https://doi.org/10.1080/15715124.2017.1411923>, 2018
- Stephens, T. A., and Bledsoe, B. P.: Probabilistic mapping of flood hazards: Depicting uncertainty in streamflow, land use, and geomorphic adjustment, *Anthropocene*, 29, 100231, <https://doi.org/10.1016/j.ancene.2019.100231>, 2020



- Stephens, T. A., and Bledsoe, B. P.: Flood Protection Reliability: The Impact of Uncertainty and Nonstationarity, *Water Resour. Res.*, 59(2), e2021WR031921, <https://doi.org/10.1029/2021WR031921>, 2023
- Rusjan, S., Vidmar, A., and Brilly, M.: The transboundary Soča and Vipava river flood problems. Paper presented at the EGU Leonardo Conference, Torino, 2012
- 510 USACE: HEC-RAS 2D User's Manual, <https://www.hec.usace.army.mil/confluence/rasdocs/r2dum/latest> (accessed August, 08-2025), 2022a
- USACE: HEC-RAS User's Manual, <https://www.hec.usace.army.mil/confluence/rasdocs/rasum/latest> (accessed August, 08-2025), 2022b
- 515 Van der Most, H., Asselman, N., and Slager, K.: Experiences in developing and applying decision support systems for strategic flood risk management, *Int. J. River Basin Manag.*, 16(3), 371-378, <https://doi.org/10.1080/15715124.2017.1411925>, 2018
- Warmink, J. J., Straatsma, M. W., and Huthoff, F.: The effect of hydraulic roughness on design water levels in river models, *Comprehensive Flood Risk Management*; Klijn, Schweckendiek, Eds.; Taylor and Francis: Abingdon, UK, 2013
- Winter, B., Schneeberger, K., Huttenlau, M., and Stötter, J.: Sources of uncertainty in a probabilistic flood risk model, *Nat. Hazards*, 91(2), 431-446, <https://doi.org/10.1007/s11069-017-3135-5>, 2018
- 520 Wright, K. A., Goodman, D. H., Som, N. A., Alvarez, J., Martin, A., and Hardy, T. B.: Improving hydrodynamic modelling: An analytical framework for assessment of two-dimensional hydrodynamic models, *River Res. Appl.*, 33(1), 170-181, <https://doi.org/10.1002/rra.3067>, 2017
- Yu, J., Li, Y., Huang, X., and Ye, X.: Data quality and uncertainty issues in flood prediction: a systematic review, *Int. J. Digit. Earth*, 18(1), 2495738. <https://doi.org/10.1080/17538947.2025.2495738>, 2025
- 525 Zahidi, I., Yusuf, B., Cope, M., Ahmed Mohamed, T., and Mohd Shafri, H. Z.: Effects of depth-varying vegetation roughness in two-dimensional hydrodynamic modelling, *Int. J. River Basin Manag.*, 16(4), 413-426, <https://doi.org/10.1080/15715124.2017.1394313>, 2018
- Zahmatkesh, Z., Han, S., and Coulibaly, P.: Understanding Uncertainty in Probabilistic Floodplain Mapping in the Time of
- 530 Climate Change, *Water*, 13(9), 1248. doi:10.3390/w13091248, 2021